Available online at www.sciencedirect.com
SCIENCE DIRECT®
Journal of Chromatography A, 996 (2003) 53–70
JOURNAL OF CHROMATOGRAPHY A
www.elsevier.com/locate/chroma

Analysis of protein adsorption on regenerated cellulose-based immobilized copper ion affinity membranes

Chun-Yi Wu[a], Shing-Yi Suen[a,*], Shiow-Ching Chen[b], Jau-Hwan Tzeng[b]

[a]*Department of Chemical Engineering, National Chung Hsing University, Taichung 402, Taiwan*
[b]*Department of Environmental Engineering, National Chung Hsing University, Taichung 402, Taiwan*

Received 21 January 2003; received in revised form 20 March 2003; accepted 20 March 2003

Abstract

Immobilized metal affinity membranes (IMAMs) were prepared by immobilizing copper ions on microporous regenerated cellulose membranes through different types of chelating agents (dentate and triazine dye). The resulting chelator utilization percentages were 95% for iminodiacetic acid, 56% for *N*,*N*,*N*-tris(carboxymethyl)ethylenediamine, 52% for Cibacron blue 3GA, and 140% for Cibacron red 3BA. On the other hand, triazine dyes were slightly superior to dentate chelators on metal ion utilization for protein adsorption. In batch single-protein adsorptions, the protein adsorption capacity decreased with increasing molecular size and number of accessible surface histidine residues [lysozyme>bovine serum albumin (BSA)>γ-globulin], while the binding strength order was the opposite (γ-globulin>BSA>lysozyme). Moreover, the proportions of specific and nonspecific bindings were evaluated by varying pH and salt concentration conditions. A large fraction of the adsorption capacity was found to come from the nonspecific interactions for the prepared IMAMs. Lastly, batch three-protein adsorptions were performed and weak adsorption competition was observed.

Keywords: Binding studies; Adsorption; Membranes; Immobilized metal affinity chromatography; Proteins

1. Introduction

In the past decade, applying affinity membranes for biomolecule separation has gained much attention owing to the lower mass-transfer limitations revealed for the membrane process than conventional column chromatography [1–4]. Various affinity modes have been adopted for membrane supports and their relative adsorption properties and separation efficiencies have been extensively investigated. Amongst the most popular affinity membrane techniques are the immobilized metal affinity membranes (IMAMs) [3–20], which are usually applied to the purification of proteins containing surface-exposed amino acids such as histidine, cysteine, tryptophan, and tyrosine, or polyhistidine-tagged biomolecules. The number of research studies on this topic has continued to increase in recent years.

The base materials for IMAMs reported in the literature [5–20] include cellulose, nylon, polysulfone, polyethylene, glass, synthetic copolymer, etc. Among these materials, cellulose membranes are a

*Corresponding author. Tel.: +886-4-2285-2590; fax: +886-4-2285-4734.
E-mail address: sysuen@nchu.edu.tw (S.-Y. Suen).

0021-9673/03/$ – see front matter
doi:10.1016/S0021-9673(03)00531-4

good choice, offering simple binding with chelating agents due to their plentiful hydroxyl groups [4]. Moreover, cellulose membranes such as cellulose acetate, cellulose nitrate, and regenerated cellulose are popular membrane materials for filtration and dialysis purposes [18] and are available commercially. In previous cellulose-based IMAM studies as reported in the review paper of Zou et al. [4], cellulose acetate and cellulose composite were used. In this study, regenerated cellulose (RC) was adopted as the solid support for IMAMs because of its low nonspecific adsorption [4,15], good chemical stability, and no prerequisite to transfer the functional groups back to hydroxyl groups as needed for cellulose acetate [11] or nitrate.

This research focused on two points. One subject was an evaluation of the effects of chelating agents for IMAM preparation, including degree of chelator utilization, the relevant stability of the immobilized metal ions, and metal ion utilization for protein adsorption. These investigations will help identify the applicability of RC-based IMAMs and explore the possible problems that may be encountered. The other aim of this work was to analyze the adsorption behavior of proteins with different numbers of surface histidines, isoelectric points, and molecular sizes, in order to distinguish the possible proportions for specific and nonspecific binding on IMAMs. This information will be useful for further improvement in the design of RC-based IMAMs.

2. Experimental

2.1. Materials

RC membranes from Sartorius (Göttingen, Germany), with a diameter of 47 mm, an average pore size of 0.45 μm, and a thickness of 160 μm, were adopted as solid supports. Cibacron blue 3GA (55% purity), Chicken egg white lysozyme [L6876, M_r 14 300, isoelectric point (pI) = 11.3], γ-globulin [G7516, basically a mixture of 80% IgG (immunoglobulin G), 10% IgM, and <10% IgA, M_r 150 000, p$I \approx 7$], and bovine serum albumin (BSA, A3059, M_r 66 000, pI = 4.7) were purchased from Sigma (St. Louis, MO, USA). Cibacron red 3BA (50% purity) was from Aldrich (Milwaukee, WI, USA). Epichlorohydrin, iminodiacetic acid, chloroacetic acid, and $CuSO_4 \cdot 5H_2O$ were obtained from Acros Organics (Geel, Belgium), TEDIA (Fairfield, OH, USA), and TCI (Tokyo, Japan).

2.2. Coupling of chelating agents

All the following reactions were conducted using a shaker at 50 rpm.

2.2.1. Dentate chelating agents: iminodiacetic acid (IDA) and N,N,N-tris(carboxymethyl)ethylenediamine (TED)

A piece of RC membrane disc was incubated in a mixed solution of 5 ml epichlorohydrin and 20 ml of 1 *M* NaOH at 60 °C for 2 h. After incubation, the membrane was rinsed with deionized (DI) water. For coupling IDA, the epichlorohydrin-conjugated membrane was reacted with 25 ml of 0.2 *M* IDA and 1 *M* Na_2CO_3, pH 11, at 80 °C for 12 h. After reaction, the membrane was washed with 5% acetic acid and then DI water. The reaction scheme is illustrated in Fig. 1a.

For coupling TED, the procedures reported in the literature [21] were followed. First, the epichlorohydrin-conjugated membrane was incubated with 5 ml ethylenediamine, pH 12, and 10 ml of 0.2 *M* $NaHCO_3$ at 80 °C for 12 h. After sequentially washing with 5% acetic acid and DI water, the membrane was reacted with 15 ml of 1 *M* chloroacetic acid and 0.2 *M* $NaHCO_3$, pH 7, at 80 °C for 12 h. After reaction, the membrane was sequentially washed with 5% acetic acid and DI water. The reaction scheme is depicted in Fig. 1b.

2.2.2. Triazine dyes [22,23]: Cibacron blue 3GA (CB 3GA) and Cibacron red 3BA (CR 3BA)

A piece of RC membrane disc was incubated in 10 ml of 3% (w/w) CB 3GA solution or 5% (w/w) CR 3BA solution at 60 °C for 30 min. After adding 10 ml of 6% (w/w) NaCl to the solution, the reaction was continued at 60 °C for 1 h. Next, 10 ml of 2% (w/w) Na_2CO_3 was added to the mixture and the temperature was raised to 80 °C. After 1 h reaction, the membrane was rinsed in DI water. The reaction schemes are shown in Fig. 2.

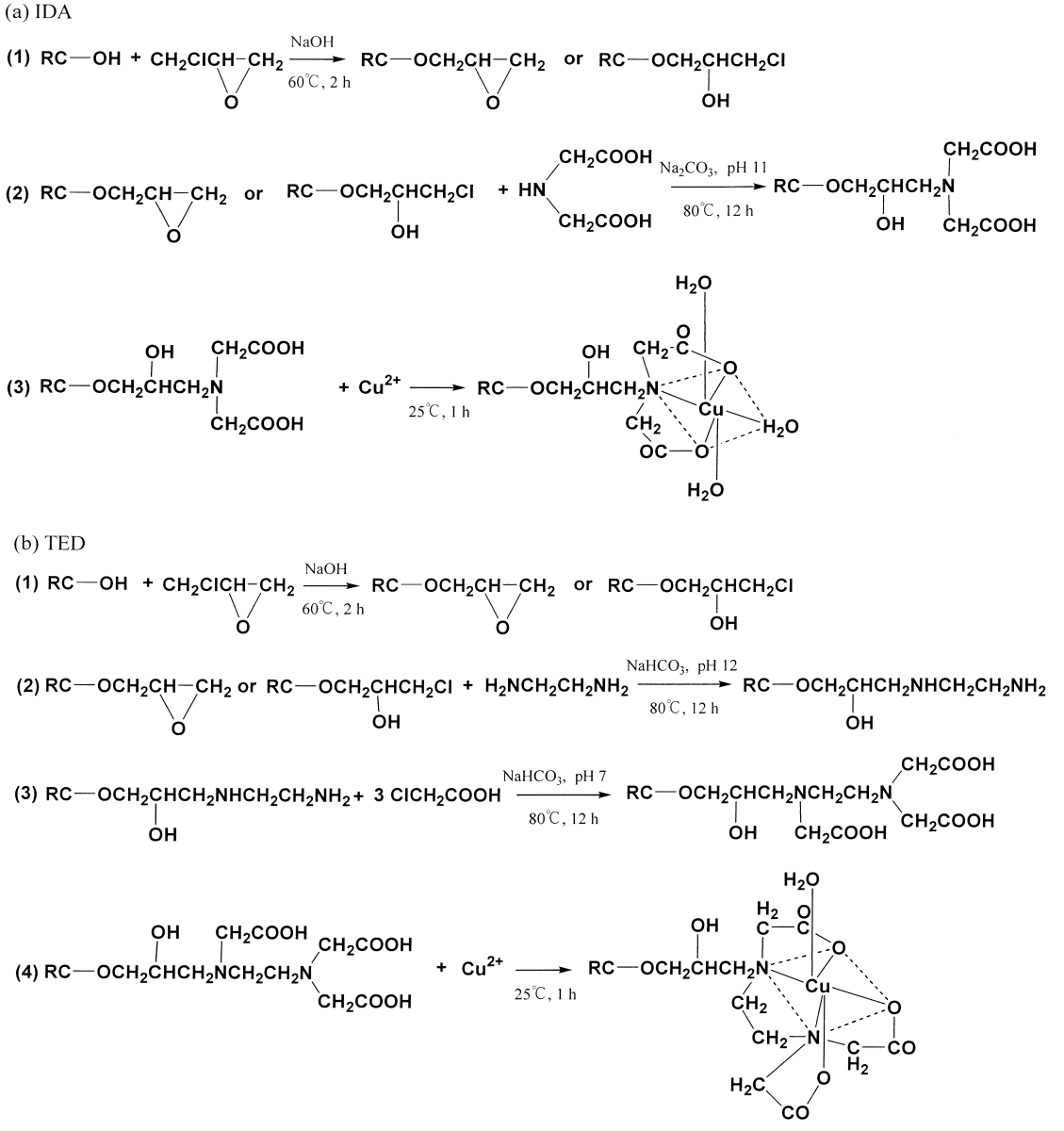

Fig. 1. Schematic diagram for the preparation of IMAMs using dentate chelators.

2.3. Determination of chelating agent capacity

2.3.1. Elemental analysis (EA)

As shown in Figs 1 and 2, all the chelating agents adopted in this work contain nitrogen. The chelating agent capacity was therefore determined by measuring the difference in nitrogen content between the epichlorohydrin-conjugated membrane and the chelating agent-coupled membrane using EA (CHNOS Rapld F002, Heraeus).

2.3.2. UV–Vis spectrophotometry: for CB 3GA capacity

A piece of CB 3GA-coupled membrane was dissolved in 5 ml of 36% (w/w) HCl. The pH was then adjusted to 7 using 6 *M* NaOH and the volume

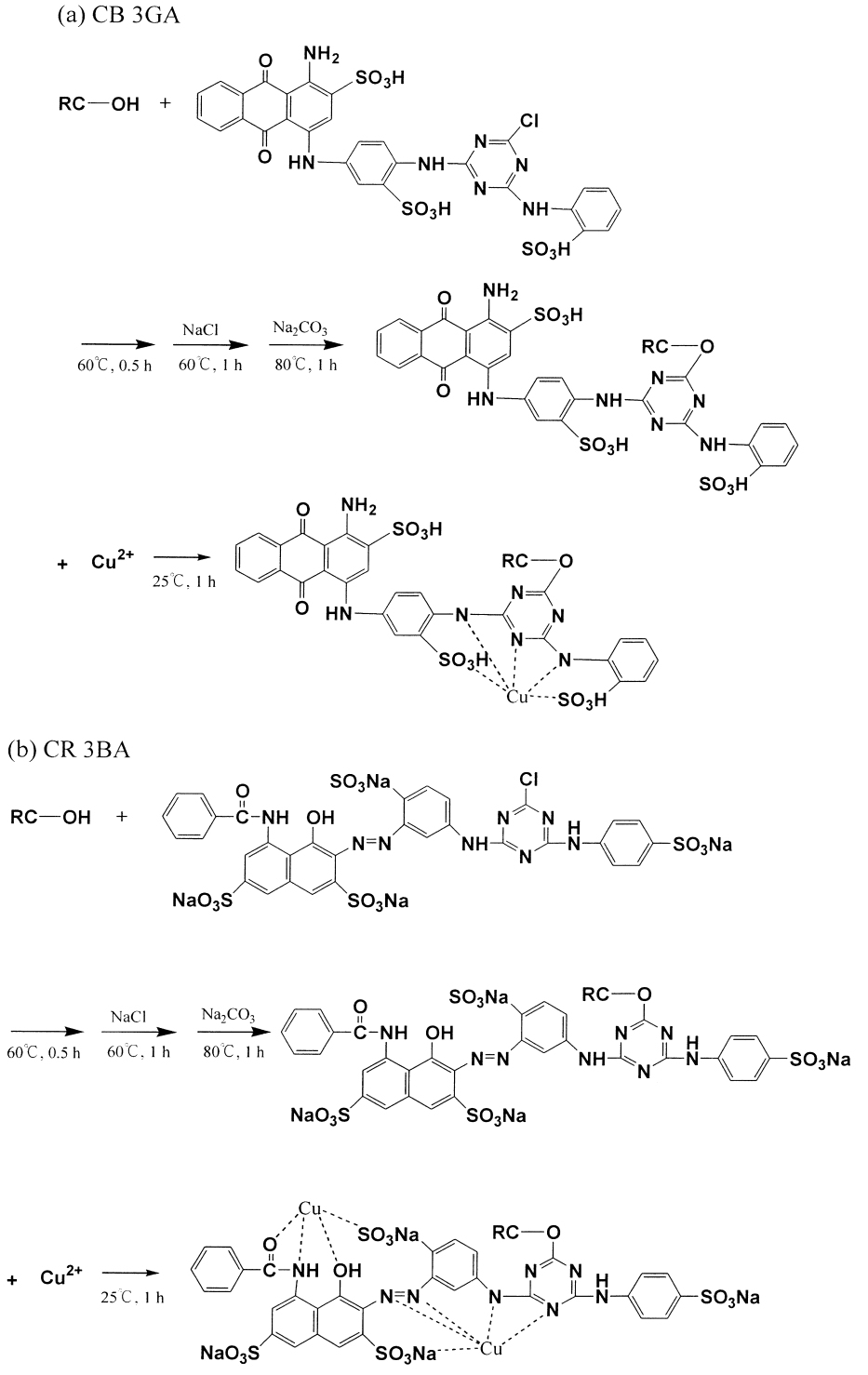

Fig. 2. Schematic diagram for the preparation of IMAMs using triazine dye chelators.

was increased to 100 ml by adding DI water. After centrifugation at 2000 rpm, the absorbance of the supernatant at 620 nm was measured using an UV–Vis instrument (UV 1601, Shimadzu). The CB 3GA concentration in the solution was obtained using the extinction coefficient of 8682 $cm^{-1}\ M^{-1}$ reported by Amersham Biosciences (Uppsala, Sweden).

2.4. Copper ion immobilization

To immobilize copper ions, a piece of chelating agent-coupled membrane was incubated with 10 ml of 0.1 *M* $CuSO_4$ solution and shaken at 50 rpm for 1 h. After incubation, the membrane was sequentially washed with DI water, 2 *M* KCl in 0.1 *M* phosphate buffer, pH 4.8, and DI water in order to remove the unbound or weakly bound copper ions. The immobilization steps for different chelating agents are depicted in Figs 1 and 2.

2.5. Determination of copper ion capacity

A piece of IMAM was suspended in 10 ml of 50 m*M* EDTA solution for 10 min to release the bound copper ions. This procedure was repeated twice to ensure that no copper ions were retained on the membrane. The copper concentration released in EDTA solution was detected using the following two methods: (1) atomic absorption spectrophotometry (AAS, Analyst 100, Perkin-Elmer); and (2) UV–Vis at 800 nm. A calibration curve for certain copper concentrations ($\leq$0.01 *M*) in 50 m*M* EDTA was employed. The immobilized copper ion capacity equals the amount released.

2.6. Batch protein adsorption

0.1 *M* Phosphate buffer was used as the loading buffer for protein adsorption. To evaluate the influence of pH, the pH values tested in this study were 9.4, 8.4, 7.4, 6.4, and 5.4. For the first two pH values tested, two of the three proteins, γ-globulin (p*I*$\approx$7) and BSA (p*I*=4.7), would be anionic and the other protein, lysozyme (p*I*=11.3), is cationic. On the other hand, one of the three proteins, BSA, would be anionic and the other two proteins, γ-globulin and lysozyme, are cationic for the last two pH values. At pH 7.4, BSA is anionic, lysozyme is cationic, and γ-globulin should be nearly neutral. In addition, for investigation of the effect of salt concentration on adsorption, 0.1, 0.5, and 1 *M* KCl in the loading buffer at pH 7.4 were adopted. The elution buffer for removing the adsorbed protein was 2 *M* KCl in 0.1 *M* phosphate buffer, pH 4.8. All the buffers were filtered through 0.2 μm cellulose acetate membranes (MFS, Osaka, Japan). Protein solutions were prepared with the loading buffer and filtered through 0.2 μm cellulose acetate filters (Millipore, Molsheim, France). All solutions were degassed prior to use.

In the batch adsorption experiment, a piece of dry affinity membrane was incubated with 5 ml protein solution of a certain concentration at room temperature for 12 h. After adsorption, the membrane was washed with loading buffer and then air-dried. Next, the membrane was rinsed twice with 5 ml of elution buffer to remove the bound protein. For regeneration, the IMAM was placed in 5 ml of 0.1 *M* $CuSO_4$ solution for 15 min to compensate for the leakage of immobilized copper ions in the previous experiment. Prior to next use, the membrane was rinsed in DI water, elution buffer, and DI water in sequence.

For single-protein adsorption, the protein concentration was measured using UV–Vis at 280 nm. The extinction coefficients (1 mg/ml) used were: 2.64 for lysozyme, 1.38 for γ-globulin (the value is actually for IgG [24]), and 0.667 for BSA. For three-protein adsorption, each protein concentration was analyzed by a LC system consisting of a peristaltic pump (AC-2120, ATTO), a UV detector (V^4, ISCO), and an anion-exchange column (Hitrap Q XL, 2.5×0.7 cm, 45–165 μm, Amersham Biosciences). The mobile phase consisted of buffer A (20 m*M* ethanolamine–HCl buffer, pH 9.5) and buffer B (1 *M* NaCl in buffer A). The flow-rate was 1 ml/min and the sample injection amount was 0.2 ml. A stepwise gradient was adopted: A–B (95:5, v/v) in 0–10 min (lysozyme peak), A–B (75:25, v/v) in 10–20 min (γ-globulin peak), A–B (50:50, v/v) in 20–30 min (BSA peak).

3. Results and discussion

3.1. Preparation of IMAMs

Two types of chelating agents, dentates (IDA and TED) and triazine dyes (CB 3GA and CR 3BA),

were employed for copper ion immobilization on the white RC membranes. Different colors were displayed for different chelating agents coupled on the RC membranes: light yellow for IDA, pale brown for TED, dark blue for CB 3GA, and bright red for CR 3BA. The membrane color turned blue after copper ion immobilization, except for the CR 3BA-coupled membranes which turned dark red. Moreover, it is impossible to distinguish the color change in the CB 3GA case, since both the dye and copper ions are blue. Through observation of membrane color changes it could be demonstrated that the RC-based IMAMs were prepared successfully. However, a strictly quantitative analysis of the chelator and copper ion capacities is still necessary for the effective application of RC-based IMAMs.

3.2. Chelating agent capacity

Chelating agent capacities obtained for the two different methods are listed in Table 1. It can be seen from the data measured by EA that chelators of similar type (i.e. dentate chelators IDA and TED, triazine dyes CB 3GA and CR 3BA) have similar capacities. Moreover, triazine dye capacities are lower than dentate capacities. This is possibly a consequence of either interference from high-percentage impurities in the dye chemicals or a microenvironmental effect of their aromatic structures, resulting in difficulty in contacting the hydroxyl groups on the RC membranes. UV–Vis chelator capacity measurement was only employed for the acid-hydrolyzed CB 3GA-coupled membranes. The result is three-fold lower than that obtained from EA measurement, although the data are of the same order of magnitude. This difference may be attributable to incomplete hydrolysis of immobilized CB 3GA.

When compared with the chelating agent capacities reported in the literature for different membrane materials (shown in Table 2), our results of 1.28 $\mu mol/cm^2$ (i.e. 80 $\mu mol/ml$ membrane volume or 173 $\mu mol/g$ dry membrane mass) for the IDA chelator and 0.52 $\mu mol/cm^2$ (i.e. 32.5 $\mu mol/ml$) for the CB 3GA chelator are superior to most reported results. For TED and CR 3BA, no relative information can be found in the literature for comparison.

3.3. Copper ion capacity

The immobilized copper ion capacities on IMAMs for different chelating agents are also presented in Table 1. The results from the two different methods were similar, but the data obtained from UV–Vis measurements were slightly lower than those from AAS measurements. The highest copper ion capacity occurred in the case of IDA. However, considering that the immobilized metal ion capacity is dependent on the coupled chelator capacity, an evaluation of chelator utilization for metal ion immobilization is more important.

In this work, the chelator utilization percentage was defined as the copper ion capacity divided by the chelating agent capacity $\times 100\%$. It was found that a high percentage of IDA (95%) was utilized, whilst only a half of TED and CB 3GA were chelated with copper. A utilization percentage higher than 100% was achieved in the case of CR 3BA. This higher-than-100% utilization can be explained from the last step illustrated in Fig. 2b, where two sites on one CR 3BA molecule are available for copper ion chelation. It should also be noted that the utilization percentage

Table 1
Chelating agent capacities and copper ion capacities for different chelating agents

Chelating agent	Chelating agent capacity ($\mu mol/cm^2$)		Copper ion capacity ($\mu mol/cm^2$)		Chelator utilization percentage[a]
	EA	UV–Vis (620 nm)	AAS	UV–Vis (800 nm)	
IDA	1.28±0.74	–	1.22±0.03	1.04±0.02	95
TED	1.11±0.57	–	0.62±0.02	0.49±0.01	56
CB 3GA	0.52±0.11	0.17±0.02	0.27±0.02	0.24±0.02	52
CR 3BA	0.50±0.15	–	0.70±0.04	0.63±0.04	140

All experiments were repeated twice.
[a] Chelator utilization percentage (%): [copper ion capacity (AAS)/chelating agent capacity (EA)]×100%.

Table 2
Chelating agent capacities, copper ion capacities, and protein binding capacities reported in the literature

Chelating agent	Membrane material	Chelating agent capacity	Copper ion capacity	Protein binding capacity	Ref.
IDA	Glycidyl methacrylate-grafted polyethylene hollow fibers	1700–1800 μmol/g base polymer	180 μmol/ml	BSA 0.26 μmol/ml	[5]
	Epoxidized polysulfone membranes	39 μmol/g[b]	41 μmol/g	–	[6]
	Sartorius membranes (170–190 μm thick)	–	65.75 μmol/cm^{2}[a]	–	[7]
	Modified glass hollow fibers	–	–	Lysozyme 69.7 mg/ml	[8]
	Glycidylether-modified polysulfone membranes	–	7.55–14.48 μmol/ml[a] (wet volume)	–	[9]
	Hydroxyethylcellulose-modified nylon membranes (150 μm thick)	–	0.17 μmol/cm^{2}	Lysozyme 300 μg/cm^{2}[b]	[10]
	Surface-modified polyethylene hollow fibers	–	1500 μmol/ml	Lysozyme 1–8.5 μmol/ml	[14]
	Polyglycidyl methacrylate-modified cotton cellulose fibers	15–150 μmol/g	–	BSA 39.09 mg/ml	[15]
	Arbor Tech microporous sheets with amine functional groups	–	800 μg/g	–	[16]
	Composite membranes of cellulose with grafted acrylic polymers	–	15.8–114.2 μmol/g[b]	–	[17]
	Polyvinyldiene fluoride-based membranes (140 μm thick)	–	0.42–0.53 μmol/cm^{2}	Lysozyme 0.055–0.085 μmol/cm^{2}	[20]
CB 3GA	Poly(2-hydroxyethyl methacrylate) membranes (ca. 600 μm thick)	1.07 μmol/cm^{2} (CB F3GA)	21.6 μg/cm^{2}	Lysozyme 165.1 μg/cm^{2}	[13]

[a] Obtained under flow mode.
[b] Obtained under flow mode with recirculation.

of TED was lower than that of IDA, which contradicts the data reported in the literature [21,25] that a pentadentate chelator (TED) should have a higher affinity for metal ions than a tridentate chelator (IDA). The worse utilization may be caused by the poorer stability of coupled TED.

When compared with the copper ion capacities listed in Table 2, our results of 1.22 μmol/cm^{2} (i.e. 76.3 μmol/ml or 165 μmol/g) for the IDA chelator and 0.27 μmol/cm^{2} (i.e. 16.9 μmol/ml) for CB 3GA are quite comparable to most reported capacities. On the other hand, the chelator utilization percentages obtained in this research, 95% for IDA and 52% for CB 3GA, are no worse than those reported in earlier work, such as 60–70% IDA utilization for grafted polyethylene hollow fibers [5], 100% IDA chelation for polysulfone-based membranes [6], and 32% CB F3GA utilization for poly(2-hydroxyethyl methacrylate) membranes [13].

3.4. Batch single-protein adsorption

3.4.1. Adsorption isotherm and effect of copper leakage

In this study, two methods were used to determine the amount of adsorbed protein in batch mode. The first method was to evaluate the difference between the amount of protein originally in the solution and that remaining after adsorption. The second method was to calculate the amount of protein eluted by multiplying the eluted concentration by the elution solution volume. As elution is complete, the amount of adsorbed protein should equal the amount eluted. The resulting adsorption isotherms (at pH 7.4) using the two methods are presented in Fig. 3. It should be noted that BSA was not adsorbed onto the IMAMs employing triazine dye chelators and therefore the results are not shown in Fig. 3 and the following related figures (e.g. Figs. 5 and 7). The negligible

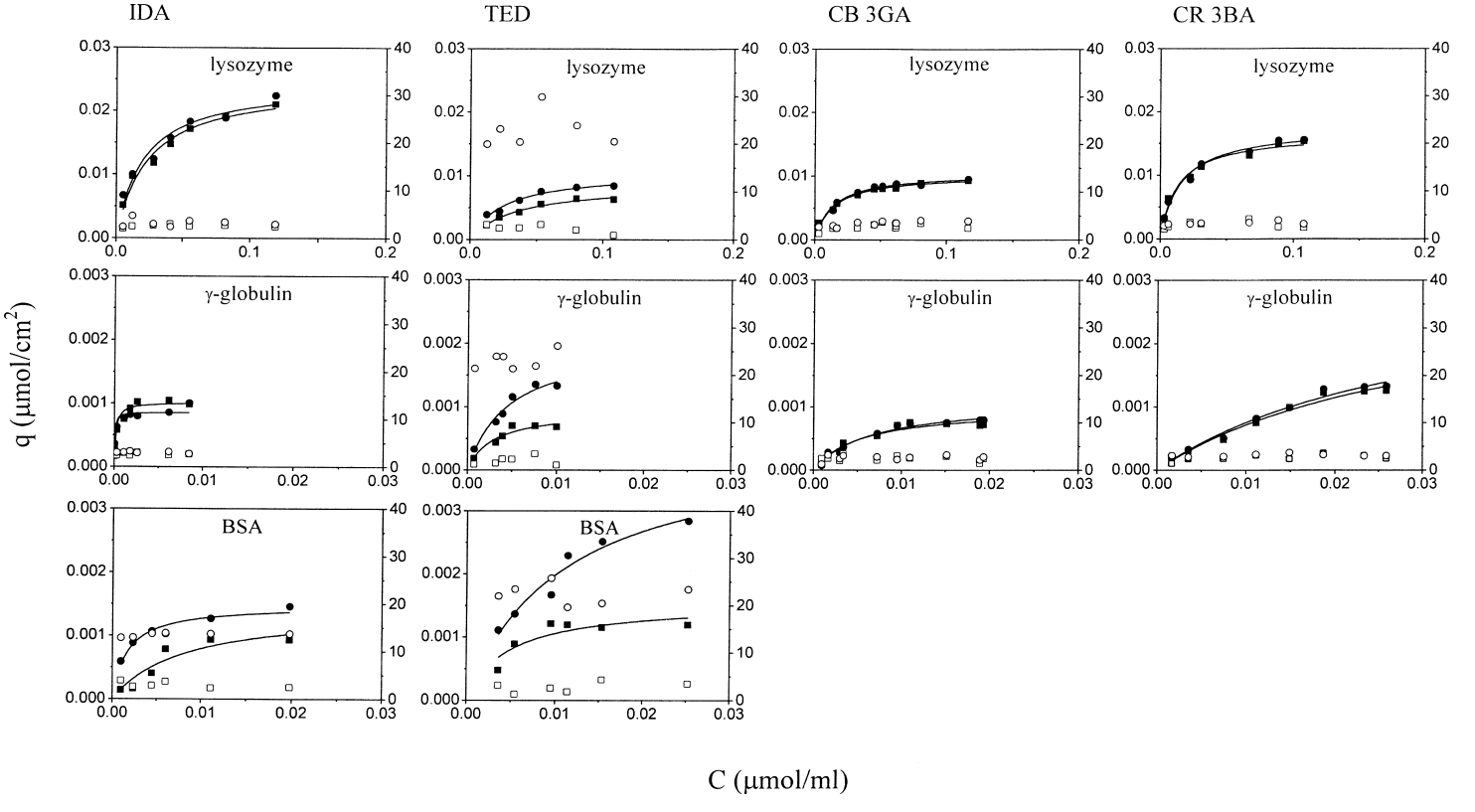

Fig. 3. Adsorption isotherms (at pH 7.4) and relevant copper leakage for different model proteins using IMAMs with different chelating agents. The adsorbed amount (q) was calculated using two methods: (■) first method (the difference between before and after adsorption); (●) second method (the amount eluted). Solid lines represent the fitted results using the Langmuir model. Copper leakage was measured at different stages: (□) at adsorption equilibrium; (○) at elution.

adsorption may be attributed to repulsion between anionic BSA molecules (at pH 7.4) and the anionic SO_3^- groups adjacent to the chelated copper ions (refer to Fig. 2).

The results in Fig. 3 show that, in some cases (e.g. CB 3GA and CR 3BA), the values determined by the different methods were in close agreement, but in other cases (e.g. TED) the difference between the two methods was significant. Moreover, in most cases the amounts adsorbed calculated using the first method were smaller than those obtained from the second method. To explain this phenomenon, the effects of copper leakage during adsorption and elution, which have been indicated as the main interfering factor for protein concentration detection in our previous study [20], were investigated.

The copper concentrations released into the solutions after each batch adsorption and elution were detected by AAS and the results are shown in Fig. 3. It was found that, in some cases (e.g. CB 3GA and CR 3BA), the released copper concentrations for adsorption and elution were very similar, but in other cases (e.g. TED) they were very different. In addition, the released copper concentrations from the adsorption stage were generally smaller than those from the elution stage. In comparison with adsorption isotherms and copper leakage results, it can be concluded that the larger adsorbed amounts obtained from the second method (i.e. the eluted protein amounts) should result from the relevantly higher leaked copper concentrations at the elution stage.

To further explore the influence on protein absorbance detection (at 280 nm) of the existence of free copper ions in solution, two cases were studied. One case was to add 5 ppm copper ions (with reference to the released copper concentrations during adsorption) to the protein solution prepared by the loading buffer; the other was to add 30 ppm copper ions (about the leaked concentrations at the elution stage) to the protein solution prepared by the elution buffer. The detected absorbances for both cases are presented in Fig. 4. The 30 ppm copper concentration significantly influenced the detection of the protein concentration. In conclusion, the method of determining the amount of adsorbed protein by evaluating the difference before and after adsorption (the first method) should be more accurate and was subsequently adopted throughout this study.

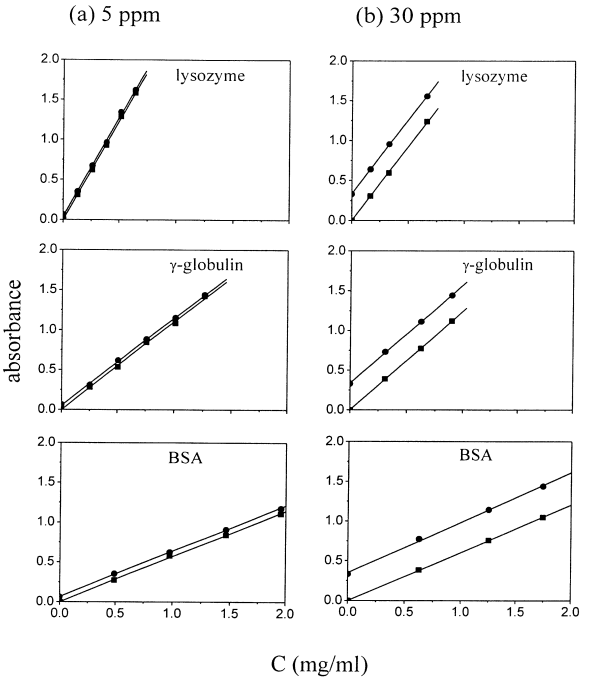

Fig. 4. Influence on the detected absorbance (at 280 nm) of the existence of free copper ions in the protein solution: (■) without copper ions; (●) with copper ions. The buffer used was: (a) loading buffer; (b) elution buffer.

There are various reasons for the copper leakage at different stages. In general, the unstably immobilized copper ions on the IMAMs may be tightly captured by protein molecules and released to the solution at the adsorption stage, whereas they are possibly displaced by high-concentration salt ions in the buffer at the elution stage. In this work, a high salt concentration was used in the elution buffer (2 *M* KCl) and may have resulted in a stronger salt displacement at the elution stage than protein capture at the adsorption stage. Consequently, copper leakage was more severe at the elution stage. However, this phenomenon is the opposite to what was found in our previous study using poly(vinylidene difluoride) (PVDF)-based membranes [20]. In that work, copper leakage was more significant at the adsorption stage (pH 7) than at the elution stage with 1 *M* KCl and pH 4. A lower salt concentration at the

elution stage appeared to reduce copper leakage. It should nevertheless be noted that, when the salt concentration in the elution buffer was reduced to 1 *M* KCl in this study, the adsorbed protein could not be completely eluted from the IMAMs. In summary, a higher salt concentration at the elution stage is more effective for increasing protein recovery, but it may also cause more severe metal ion leakage from the IMAMs. An appropriate salt concentration should be carefully selected.

According to the chelating mechanism shown in Fig. 1, the pentadentate chelator TED should bind more strongly to metal ions than the tridentate IDA, which would ensure a better stability of the chelate complex and hence a lower metal ion leakage [21,25]. However, as shown in Fig. 3, the use of TED caused a large copper leakage. This contradiction also reveals the failure to form a stable metal chelate structure with TED on RC membranes. In addition, the released copper concentrations reported in this work are higher than those reported for cellulose acetate-based IMAMs [11]. Further improvement in the prevention of metal ion leakage for RC-based IMAMs is imperative.

3.4.2. Copper utilization percentage

The single-protein isotherms presented in Fig. 3 were fitted by the Langmuir isotherm model, $q = q_m C/(K_d + C)$, where q_m represents the saturation capacity and K_d is the dissociation equilibrium constant. The fitted parameters are listed in Table 3. The results show that lysozyme has the highest saturation capacity and copper utilization percentage, while γ-globulin has the lowest values. The decrease in protein binding capacity with increase in molecular size (the order of molecular size is γ-globulin > BSA > lysozyme) may be explained by the possibility that the binding of a large protein molecule blocks the access to multiple metal ion sites on the IMAMs [14,26]. Moreover, γ-globulin (mainly IgG) has several accessible surface histidine residues [27,28], while lysozyme and BSA have only one or two to three exposed histidines [25,26]. Multipoint attachment is another possible cause of the lower ligand utilization, especially for γ-globulin.

As shown in Table 3, triazine dye chelators have higher copper utilization percentages than dentate chelators, although all the values are low. When compared with the data reported in the literature (refer to Table 2), the saturation capacities and metal ion utilization percentages obtained in this research lie between the results from previous studies. Nevertheless, in the case of CB 3GA, both the lysozyme capacity and copper utilization fraction are greater than those for poly(HEMA) membranes [13].

Another important isotherm parameter presented in Table 3 is the dissociation equilibrium constant. In most cases, the order of the K_d value was

Table 3
Langmuir isotherm parameters and copper utilization percentages for different chelating agents and different model proteins

Chelating agent	Model protein	Langmuir isotherm parameters		R^2	Copper utilization percentage[a]
		q_m (μmol/cm^2)	K_d (μmol/ml)		
IDA	Lysozyme	0.0244±0.0016	0.0234±0.0047	0.97	2.0
	γ-Globulin	0.0010±0.0001	0.0020±0.0001	0.86	0.08
	BSA	0.0015±0.0004	0.0083±0.0051	0.88	0.12
TED	Lysozyme	0.0086±0.0006	0.0333±0.0058	0.98	1.4
	γ-Globulin	0.0009±0.0001	0.0028±0.0012	0.92	0.14
	BSA	0.0016±0.0002	0.0046±0.0024	0.78	0.26
CB 3GA	Lysozyme	0.0103±0.0003	0.0139±0.0019	0.98	3.8
	γ-Globulin	0.0010±0.0001	0.0053±0.0014	0.94	0.37
	BSA	–	–	–	–
CR 3BA	Lysozyme	0.0165±0.0008	0.0130±0.0024	0.98	2.4
	γ-Globulin	0.0029±0.0006	0.0304±0.0103	0.98	0.41
	BSA	–	–	–	–

[a] Copper utilization percentage (%): [q_m/copper ion capacity (AAS)]×100%.

lysozyme>BSA>γ-globulin. Since the inverse of K_d represents the binding strength, this implies that the order of the binding strength with the immobilized copper ions on the IMAMs was γ-globulin> BSA>lysozyme. Considering the number of exposed histidine residues for these three proteins, multipoint binding would be the most probable reason for the strong binding of γ-globulin.

3.4.3. Nonspecific binding

The possible mechanisms for protein adsorption onto the IMAMs are categorized into four types of interactions [10,20,21,26,29]: (1) the affinity binding provided by the electron-donating capacity of the imidazole groups of the exposed histidine residues on the protein surface with the immobilized metal ions; (2) the electrostatic interaction between the charged protein molecules and positively charged metal ions; (3) the electrostatic interaction between the charged protein molecules and the negatively charged sites on the membrane surface, such as the unreacted hydroxyl groups from the basic cellulose materials, the residual carboxyl groups for dentate chelators, or the residual SO_3^- groups for triazine dye chelators; and (4) the hydrophobic interaction between the protein and the hydrophobic sites on the membrane surface. The former two interactions contribute to the specific binding between protein and immobilized ligand, whereas the latter two are nonspecific bindings.

This section reports on the nonspecific binding of protein to the membranes. Blank RC membranes and the membranes from each intermediate reaction step before complete metal ion immobilization were employed in batch single-protein adsorption (pH 7.4). The nonspecific binding results and the relevant adsorptions on the IMAMs at high feed concentrations are presented in Fig. 5. For triazine dye chelators, BSA adsorptions are not shown in the figure, since BSA was neither adsorbed onto the triazine dye-bound membranes nor onto the relevant IMAMs. The reason for this has been described above.

As mentioned previously, nonspecific binding consists of electrostatic and hydrophobic interactions. At pH 7.4, lysozyme (pI=11.3) is cationic, γ-globulin (pI=7) is slightly cationic, and BSA (pI=4.7) is anionic. Since the residual charged groups on the chelator-coupled membranes are anionic, only the electrostatic interaction between cationic lysozyme and the chelator-coupled membranes is significant. This explains why lysozyme adsorption onto the chelator-coupled membranes was significantly increased compared with the results for blank RC membranes or the membranes from an earlier reaction step, as shown in Fig. 5. For γ-globulin and BSA, their adsorption onto the chelator-coupled membranes was similar to that for blank membranes or the membranes from an earlier step. Nonspecific electrostatic interactions were not dominant in these cases.

3.4.4. Salt concentration effect

Fig. 6 shows the salt concentration effect on lysozyme and γ-globulin adsorption at pH 7.4. The results for BSA are not presented because adsorption became practically negligible once a low salt concentration such as 0.1 *M* KCl was added. For most cases in Fig. 6, lysozyme and γ-globulin adsorptions are greatly reduced when 0.1 *M* KCl was added and then continue to decrease until the salt concentration was increased to 0.5 *M*. Above 0.5 *M*, a further increase in salt concentration hardly altered the adsorption capacities.

The salt concentration effects on the four types of interactions can be explained as follows. With increasing salt concentration, the affinity binding between the exposed histidine residues of the protein and the immobilized metal ions would hardly be affected [29], same as for the specific binding electrostatic interaction since both lysozyme and γ-globulin are cationic at pH 7.4 and exhibit repulsive interactions with cationic copper ions. For nonspecific binding, the attraction for cationic proteins with negatively charged groups on the IMAMs would be reduced with increasing salt concentration, but the strength of the hydrophobic interaction should be enhanced [29]. As shown in Fig. 6, protein adsorption was significantly decreased after the addition of 0.1 *M* KCl, indicating that the nonspecific electrostatic interaction was dominant. When the salt concentration was further increased, the effect of the nonspecific hydrophobic interaction would compensate for the effect of the nonspecific electrostatic interaction. This is why the protein adsorption capacities are unchanged for salt con-

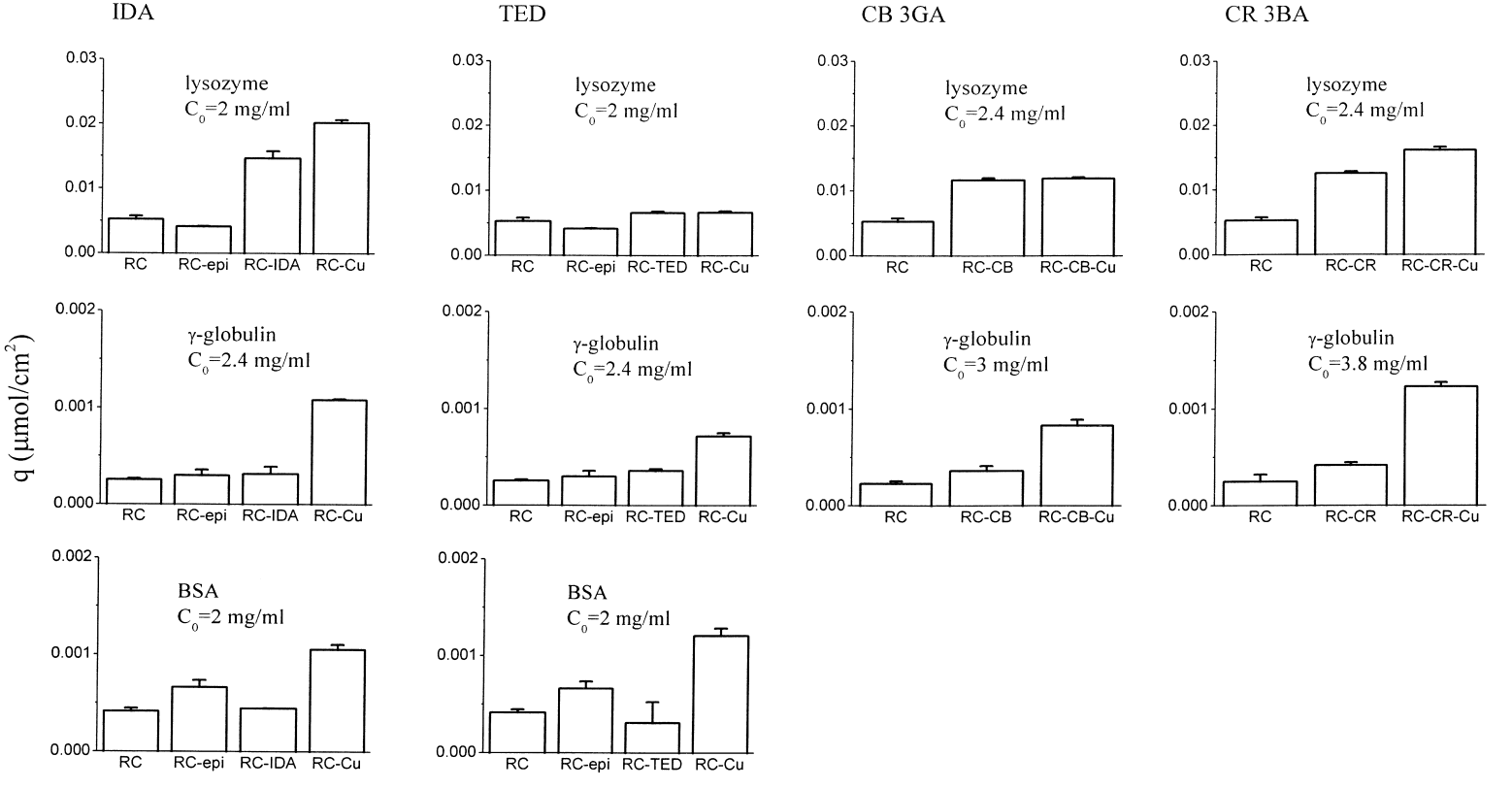

Fig. 5. Nonspecific binding of different model proteins to blank RC membranes and the membranes from each intermediate reaction step in comparison with adsorption on the IMAMs.

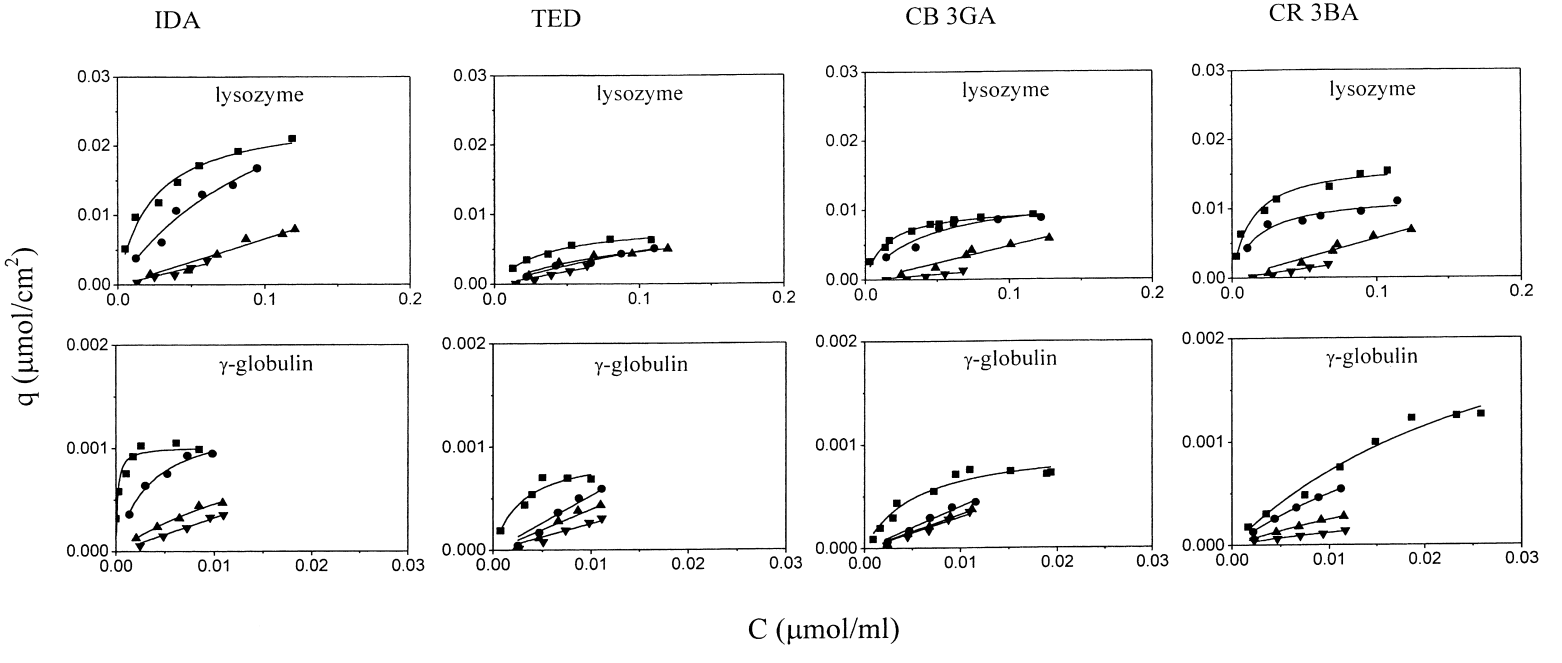

Fig. 6. Adsorption isotherms (at pH 7.4) with various KCl concentrations for different model proteins using IMAMs with different chelating agents: (■) no KCl, (●) 0.1 *M* KCl, (▲) 0.5 *M* KCl, (▼) 1 *M* KCl. Solid lines represent the fitted results using the Langmuir model.

centrations above 0.5 *M*. The unchanged capacity indicates a specific binding capacity. On the other hand, BSA is anionic at pH 7.4 and its specific electrostatic interaction with cationic copper ions would be greatly reduced with increasing salt concentration. Consequently, BSA adsorption is negligible at a low salt concentration such as 0.1 *M*.

Fractions of residual hydroxyl groups from base cellulose material and unreacted epichlorohydrin on the IMAMs were not examined in this study. If only the unbound chelator percentage was taken into account, the proportion of nonspecific binding sites should be low for the IMAMs with IDA and CR 3BA chelators. However, the above analysis of the salt concentration effect implies that the nonspecific binding proportion for these two IMAMs was still relatively high, which may not only be a result of incomplete chelator utilization. Therefore, a detailed evaluation of the degree of conversion for each reaction step in the process of IMAM preparation is needed.

3.4.5. pH effect

The adsorption results as a function of pH (from 5.4 to 9.4) are presented in Fig. 7. Lysozyme adsorption increased with increasing pH, irrespective of the chelating agent employed. γ-Globulin adsorption increased with increasing pH from 5.4 to 7.4 (or 8.4) and then decreased when the pH was raised further (γ-globulin was not adsorbed onto the IMAMs with TED at pH 5.4). The pH effect on BSA adsorption is similar to that for γ-globulin adsorption, but BSA adsorption decreased at lower pH (ca. pH 7.4).

To determine the dominating binding force for each protein, the possible variations for each type of interaction with changing pH need to be examined. The specific binding effects can be analyzed as follows. First, partial deprotonation of the exposed histidine residue of the protein would be promoted by increasing pH in the range higher than its pK_a (about 6–7 [30]), which would increase the possibility of specific binding with immobilized cationic copper ions [29]. Except for pH 5.4, the pH values adopted in this work are higher than the pK_a of the histidine residue. Therefore, affinity binding between the histidine residues of the protein and the IMAMs should have increased with increasing pH and hence resulted in higher adsorption capacities. In this respect, all three proteins should exhibit similar behavior. Secondly, the electrostatic interaction between the charged protein and the immobilized cationic copper ions is repulsive for a cationic protein and attractive for an anionic protein. In the pH range 5.4–9.4, lysozyme (pI = 11.3) is cationic, γ-globulin (pI = 7) is cationic below pH 7 and anionic above pH 7, and BSA (pI = 4.7) is anionic. With increasing pH, a cationic protein would become less cationic and an anionic protein would become more anionic, which would lead to reduced repulsion or increased attraction for the immobilized cationic copper ions. Protein binding via this type of electrostatic interaction would accordingly be enhanced, even though the molecular charge is different for different proteins. Summing up the above analyses, both types of specific interactions would be improved with increasing pH in the case of all three proteins.

With respect to nonspecific binding, one mechanism is the electrostatic interaction between the charged protein and the negatively charged groups remaining on the IMAMs such as carboxyl groups for dentate chelators (p$K_a \approx 3$ [31,32]) and SO_3^- groups for triazine dye chelators (pK_a = 3–4 [32]). The pH range used in this work is higher than the pK_a values of these residual groups. With increasing pH, the cationic lysozyme would become less cationic, but the residual negatively charged groups on the membranes would be more anionic. Their electrostatic interaction would change very little [29]. On the other hand, with a high pI (ca. 11.3), lysozyme would possess a higher degree of neutrality at higher pH and its hydrophobic interaction with the IMAMs might be improved [29]. The increased lysozyme adsorption with increasing pH shown in Fig. 6 could therefore be attributed to all the enhancing effects on most types of interactions, except for the nonspecific electrostatic interaction.

For the same reasons as for lysozyme, below pH 7 the nonspecific electrostatic interaction between the cationic γ-globulin and the anionic residual groups of the IMAMs would hardly vary, but the hydrophobic interaction would increase with increasing pH. Therefore, γ-globulin adsorption would improve with increasing pH in this pH range. With the pH above 7, γ-globulin becomes anionic. Both γ-

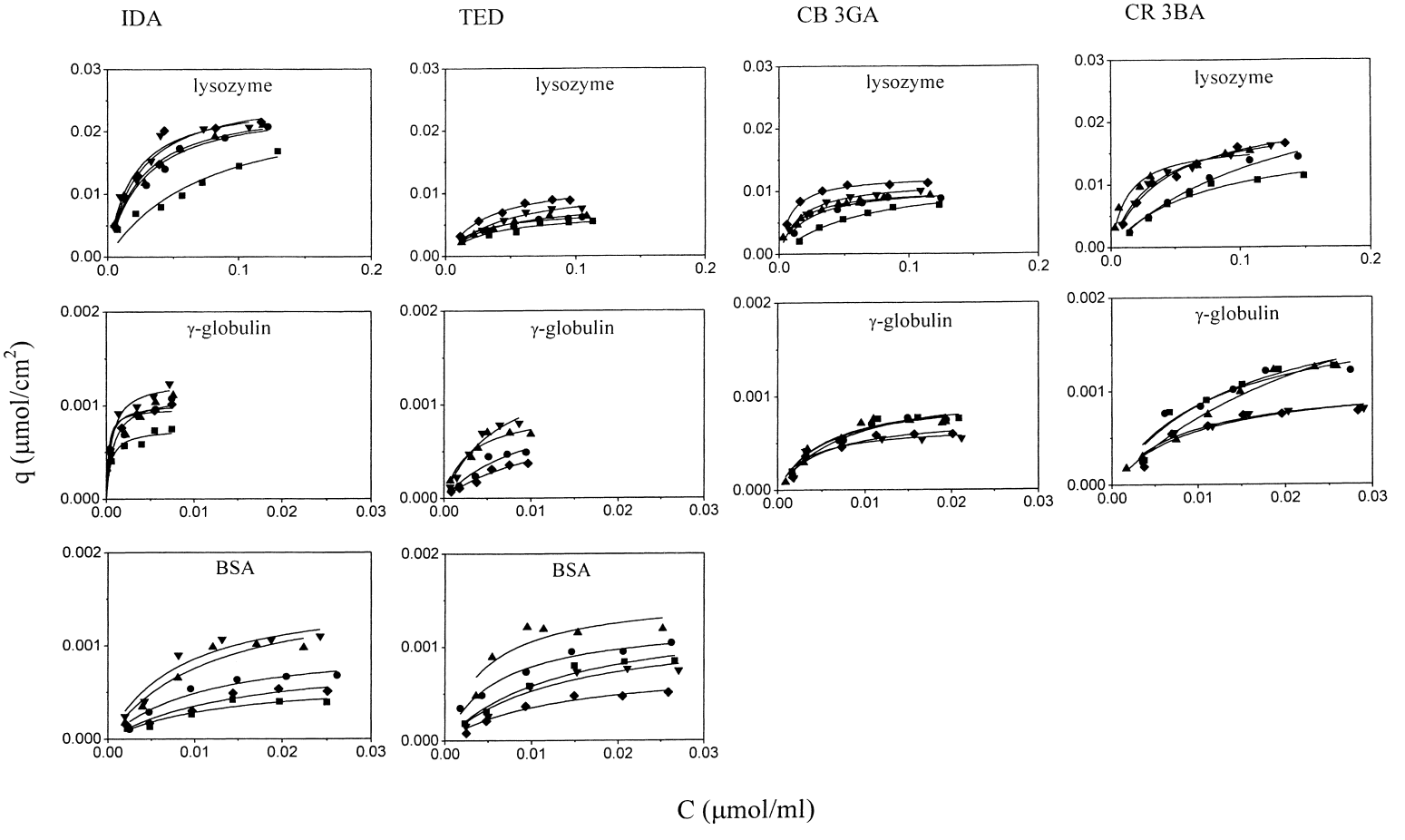

Fig. 7. Adsorption isotherms at various pH values for different model proteins using IMAMs with different chelating agents: (■) pH 5.4, (●) pH 6.4, (▲) pH 7.4, (▼) pH 8.4, (♦) pH 9.4. Solid lines represent the fitted results using the Langmuir model.

globulin and the negatively charged groups on the IMAMs would become more anionic with increasing pH, which would cause repulsion and eventually lead to a declining adsorption. On the other hand, the hydrophobic interaction between γ-globulin and the IMAMs would be reduced with increasing pH in this range because γ-globulin becomes more and more nonneutral. When the decreasing effect from both nonspecific bindings is more significant than the improving effect from both specific bindings, γ-globulin adsorption would be decreased. This explains why γ-globulin adsorption was reduced at pH 8.4 for triazine dye chelators and at pH 9.4 for dentate chelators.

With respect to BSA, it is always anionic in the pH range used in this study. For the same reasons as for γ-globulin adsorption at pH >7, BSA adsorption would also decrease with increasing pH when the nonspecific binding effects are more dominant than the specific binding effects. This is shown by the results for pH >7.4.

3.5. Batch three-protein adsorption

Competitive adsorption behavior for the IMAM technique may occur when several proteins with different affinities coexist in solution. To investigate this effect, batch three-protein adsorptions were conducted using the IMAMs with the IDA chelator, and the isotherm results are shown in Fig. 8. γ-Globulin reached its saturation capacity at the lowest equilibrium concentration, implying that γ-globulin should have the strongest binding with the IMAMs among these three proteins. This result agrees with that for the batch single-solute adsorptions. On the other hand, lysozyme and BSA exhibited slightly lower saturation capacity and weaker binding (saturation was attained at a higher equilibrium concentration) than in the single-solute cases. Summing up these findings, weak adsorption competition occurred for the three proteins together, but it was ineffective to accomplish a clear separation of these proteins.

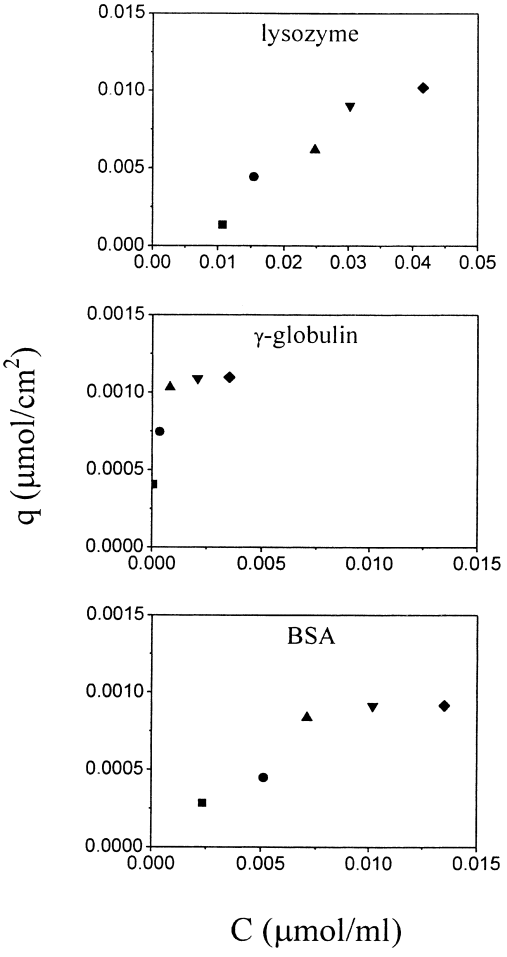

Fig. 8. Three-protein adsorption isotherms using the IMAMs with the IDA chelator. C_0 for three model proteins: (■) 0.22 mg/ml, (●) 0.44 mg/ml, (▲) 0.66 mg/ml, (▼) 0.88 mg/ml, (♦) 1.10 mg/ml.

4. Conclusions

Because of its low nonspecific protein adsorption and no need to transfer the functional groups back to hydroxyl groups before ligand immobilization as compared with other cellulose compounds, regenerated cellulose membranes were selected as the base materials for the preparation of IMAMs in this study. Using different types of chelating agents, microporous RC membranes were immobilized with copper ions. Chelator effects were investigated systematically by analyzing the chelator capacity, the immobilized metal ion capacity, and the protein adsorption capacity under identical experimental conditions. The results show that triazine dyes are slightly

superior to dentate chelators with respect to copper ion utilization for protein adsorption, although some dentate chelators such as IDA provided a higher chelator utilization for copper ion immobilization. Either steric crowding or multipoint attachment may have reduced the immobilized metal ion utilization.

The active groups on the base membrane material, the membrane shape, the nature of the chelating agent, the immobilization method, the type of metal ion, and the metal ion concentration all play an important role in determining the immobilized metal ion capacity for IMAMs. In this study, the only condition changed was the chelator, but the resulting metal ion and protein capacities were very different for the various chelators. This information will be important for the design of RC membranes to serve as IMAMs. When using IDA or CB 3GA as the chelator, the resulting chelator capacity and copper ion capacity obtained in this work are comparable to most reported IMAM results. However, in order to be superior to other cellulose-based or other polymer-based IMAMs, how to increase both the chelator and copper ion capacities for RC-based IMAMs is a vital issue. In recent research of the present authors, an increase in the shaking rate for the whole procedure, including chelator coupling and metal ion immobilization, was found to be a key factor for achieving higher capacities, and the results of that work will be published in the near future [33].

Batch single-protein adsorptions onto RC-based IMAMs for three model proteins with different molecular sizes and isoelectric points were also evaluated in this work. The fractions of specific and nonspecific interactions were distinguished by varying the pH and salt concentration. The results imply that, even though blank RC membranes display low nonspecific binding, a large proportion of the adsorption capacity of RC-based IMAMs originated from nonspecific interactions, which may reduce their applicability. To resolve this problem, more detailed analyses of the conversion ratio for each single reaction step are being conducted in our laboratory and a suitable method for blocking the unreacted residual groups is being examined. In addition, to evaluate the applicability of RC-based IMAMs, a test of membrane reusability is also required, and this was done by reusing the same piece of IMAM to adsorb the same protein at the same initial concentration several times. The data (not shown) were found to be reproducible (the error was below 7%). Finally, to exploit the practical applicability of these RC-based IMAMs, their application to the purification of valuable enzymes and histidine-tagged viruses is being examined and the results will be published in the near future [33].

Acknowledgements

The authors would like to thank Mr. Ching-Lung Chen for his help with the analysis of the copper ion concentration by AAS.

References

[1] S. Brandt, R.A. Goffe, S.B. Kessler, J.L. O'Connor, S.E. Zale, Biotechnology 6 (1988) 779.
[2] D.K. Roper, E.N. Lightfoot, J. Chromatogr. A 702 (1995) 3.
[3] C. Charcosset, J. Chem. Technol. Biotechnol. 71 (1998) 95.
[4] H. Zou, Q. Luo, D. Zhou, J. Biochem. Biophys. Methods 49 (2001) 199.
[5] H. Iwata, K. Saito, S. Furusaki, T. Sugo, J. Okamato, Biotechnol. Prog. 7 (1991) 412.
[6] K. Rodemann, E. Staude, J. Membr. Sci. 88 (1994) 271.
[7] O.-W. Reif, V. Nier, U. Bahr, R. Freitag, J. Chromatogr. A 664 (1994) 13.
[8] G.C. Serafica, J. Pimbley, G. Belfort, Biotechnol. Bioeng. 43 (1994) 21.
[9] K. Rodemann, E. Staude, Biotechnol. Bioeng. 46 (1995) 503.
[10] T.C. Beeskow, W. Kusharyoto, F.B. Anspach, K.H. Kroner, W.-D. Deckwer, J. Chromatogr. A 715 (1995) 49.
[11] N. Kubota, Y. Nakagawa, Y. Eguchi, J. Appl. Polym. Sci. 62 (1996) 1153.
[12] M.Y. Arica, H.N. Testereci, A. Denizli, J. Chromatogr. A 799 (1998) 83.
[13] A. Denizli, S. Senel, M.Y. Arica, Colloids Surfaces B 11 (1998) 113.
[14] S.A. Camperi, M. Grasselli, A.A. Navarro del Canizo, E.E. Smolko, O. Cascone, J. Liq. Chromatogr. Relat. Technol. 21 (1998) 1283.
[15] L. Yang, L. Jia, H. Zou, D. Zhou, Y. Zhang, Sci. China, Ser. B: Chem. 41 (1998) 596.
[16] J. Crawford, S. Ramakrishnan, P. Periera, S. Gardner, M. Coleman, R. Beitle, Sep. Sci. Technol. 34 (1999) 2793.
[17] L. Yang, L. Jia, H. Zou, Y. Zhang, Biomed. Chromatogr. 13 (1999) 229.
[18] P.R. Hari, W. Paul, C.P. Sharma, J. Biomed. Mater. Res. 50 (2000) 110.

[19] S. Senel, R. Say, M.Y. Arica, A. Denizli, Colloids Surfaces A 182 (2001) 161.
[20] Y.-H. Tsai, M.-Y. Wang, S.-Y. Suen, J. Chromatogr. B 766 (2002) 133.
[21] J. Porath, B. Olin, Biochemistry 22 (1983) 1621.
[22] H.-C. Liu, J.R. Fried, AIChE J. 40 (1994) 40.
[23] S.-Y. Suen, S.-Y. Lin, H.-C. Chiu, Ind. Eng. Chem. Res. 39 (2000) 478.
[24] F.W. Putnam, in: F.W. Putnam (Ed.), 2nd ed., The Plasma Proteins: Structure, Function, and Genetic Control, Vol. 1, Academic Press, New York, 1975, p. 62.
[25] V. Gaberc-Porekar, V. Menart, J. Biochem. Biophys. Methods 49 (2001) 335.
[26] S. Sharma, G.P. Agarwal, Anal. Biochem. 288 (2001) 126.
[27] J. Hale, D. Biedler, Anal. Biochem. 222 (1994) 29.
[28] G. Tishchenko, J. Dybal, K. Meszarosova, Z. Sedlakova, M. Bleha, J. Chromatogr. A 954 (2002) 115.
[29] W.-Y. Chen, C.-F. Wu, C.-C. Liu, J. Colloid Interface Sci. 180 (1996) 135.
[30] F.H. Arnold, Biotechnology 9 (1991) 151.
[31] Z. El Rassi, Cs. Horvath, J. Chromatogr. 359 (1986) 241.
[32] D.R. Lide (Ed.), CRC Handbook of Chemistry and Physics, 83rd ed., CRC Press, New York, 2002, p. 46.
[33] Y.-C. Liu, C.-C. ChangChien, S.-Y. Suen (submitted for publication).